

Article

Generic Behavior of Electromagnetic Fields of Regular Rotating Electrically Charged Compact Objects in Nonlinear Electrodynamics Minimally Coupled to Gravity

Irina Dymnikova * and Evgeny Galaktionov

A.F. Ioffe Physico-Technical Institute of the Russian Academy of Sciences, Polytekhnicheskaja 26, 194021 St. Petersburg, Russia

* Correspondence: igd.ammp@mail.ioffe.ru or irina@uwm.edu.pl; Tel.: +7-812-292-7912

Abstract: Regular rotating electrically charged compact objects are described by nonlinear electrodynamics minimally coupled to gravity in a self-consistent way and without additional assumptions on the relation between the electromagnetic field and gravity. The electromagnetic fields obey the system of four source-free nonlinear equations for the electromagnetic tensor $F_{\mu\nu}$, with only two independent components due to spacetime symmetry determined by the algebraic structure of electromagnetic stress–energy tensors ($p_r = -\rho$). In this paper, we present, for an arbitrary gauge-invariant Lagrangian, the general regular solution and generic behavior of electromagnetic fields, including the generic features of the Lagrange dynamics, for regular rotating electrically charged black holes and electromagnetic spinning solitons.

Keywords: regular electrically charged rotating black hole; electromagnetic spinning soliton; electromagnetic fields



Citation: Dymnikova, I.; Galaktionov, E. Generic Behavior of Electromagnetic Fields of Regular Rotating Electrically Charged Compact Objects in Nonlinear Electrodynamics Minimally Coupled to Gravity. *Symmetry* **2023**, *15*, 188. <https://doi.org/10.3390/sym15010188>

Academic Editor: Jeffery Secrest

Received: 14 December 2022

Revised: 31 December 2022

Accepted: 5 January 2023

Published: 9 January 2023



Copyright: © 2023 by the authors. Licensee MDPI, Basel, Switzerland. This article is an open access article distributed under the terms and conditions of the Creative Commons Attribution (CC BY) license (<https://creativecommons.org/licenses/by/4.0/>).

1. Introduction

Nonlinear electrodynamics minimally coupled to gravity (NED-GR) describes, in a self-consistent way and without additional assumptions concerning NED-GR coupling, generic properties of regular electrically charged black holes and electromagnetic solitons replacing naked singularities as non-dissipated compact objects related by electromagnetic and gravitational interaction.

The physical mechanisms responsible for the existence of astrophysical electrically charged black holes have been considered in the literature during almost half a century. In 1974, it has been shown that a black hole with the angular momentum J in an external magnetic field B captures charged particles up to acquiring the charge $q = 2BJ$ [1]. Mechanisms of black hole charging in the process of its interaction with the ionized cosmic plasma in the magnetic field has been presented and analyzed in [2]. The self-consistent analysis of accretion of a collisionless charged fluid on a neutral black hole, carried out in [3], has resulted in the estimate of an acquired charge $0 < q/m < 0.99$. The method of testing an astrophysical black hole for the existence of a charge by using the process of reflection of electromagnetic waves has been proposed in [4].

The idea of an electromagnetic spinning soliton goes back to the early classical models of the electron, visualized as an extended spherical electrically charged particle with the finite energy. The necessary condition for its existence, formulated by Abraham [5] and Lorentz [6,7], required introducing an *ad hoc* additional cohesive force of the non-electromagnetic origin to prevent an extended charged electron from scattering apart under the Coulomb repulsion. Analyzing models of this type, Dirac did not find physical reasons for the proposed assumptions concerning the character and origin of an additional non-electromagnetic force [8].

At the same time, development of point-like models of spinning particles gradually involved and developed instruments needed for description of an extended particle, and led to the Dirac nonlinear electrodynamics [9] (for a brief description of this story, see [10]).

In the 1962 Dirac model, the electron was visualized as an electrically charged surface, with zero electromagnetic field inside, the external field, determined by the surface Maxwell equations, and a needed non-electromagnetic force provided by a surface tension [11]. In General Relativity, the extended models have been presented by Boyer for rotating fluid masses [12,13]. It was shown that a perfect-fluid interior can be matched to any given exterior field, and the boundary conditions were formulated for all possible isolated, axially symmetric, uniformly rotating perfect-fluid mass configurations in a steady state [12,13].

In 1982, Righi and Venturi found that the Dirac nonlinear electrodynamics admits the spherically symmetric static solutions of an extended type, which can be applied for modeling a charged particle [14]. In 1993, a generalization of the Dirac nonlinear electrodynamics was proposed [15], which admits a soliton-like solution, equipped with the Coulomb field and the field of a magnetic dipole, appropriate for description of a charged particle. The soliton mass is finite; the angular momentum, stored in its electromagnetic field, has been associated with the particle spin. A charged spinning soliton is visualized as a sphere of the radius r_e introduced for dimensional reason; the magnetic momentum μ_e and the electric charge e come as constants of integration. The soliton-type behavior is manifested by the complete accessibility of a particle interior to another particle, neutral or charged with the same sign [15]. Contemporary models developed on the basis of spin dynamics are presented in [16,17] (for a recent review, see [10]).

Another road has been opened in 1965 by the Kerr–Newman geometry which describes the rotating electrically charged objects in the linear electrodynamics coupled to gravity, by the electrovacuum solution to the Einstein–Maxwell equations with the metric [18]

$$ds^2 = -dt^2 + \frac{\Sigma}{\Delta} dr^2 + \Sigma d\theta^2 + \frac{(2mr - q^2)}{\Sigma} (dt - a \sin^2 \theta d\phi)^2 + (r^2 + a^2) \sin^2 \theta d\phi^2; \quad (1)$$

$$\Sigma = r^2 + a^2 \cos^2 \theta; \quad \Delta = r^2 - 2mr + a^2 + q^2, \quad (2)$$

where m is the mass, q is the electric charge, and a is the angular momentum. The electromagnetic potential is given by [18]

$$A_i = -(q/r)\Sigma[1; 0, 0, -a \sin^2 \theta]. \quad (3)$$

In 1968, Carter has reported that the parameter a coupled with the mass m gives the angular momentum $J = ma$, and coupled with the charge q gives an asymptotic magnetic momentum $\mu_q = qa$, and the same gyromagnetic ratio as predicted by the Dirac equation for a spinning particle [19]. This gave rise to search for models of internal sources of the Kerr–Newman fields motivated by the construction of a model for the electron as a charged spinning structure without horizons $r_{\pm} = m \pm \sqrt{m^2 - (a^2 + q^2)}$, when $a^2 + q^2 > m^2$. In this case, however, $g_{\phi\phi} < 0$ for $2mr < q^2$ which leads to causality violation, i.e., the existence of closed time-like curves, originated in the interior region $r < q^2/2m$, and extended over the whole manifold [19].

The models of a matter source for the Kerr–Newman fields, based on screening or covering the causally dangerous region, include disk-like [20–22], shell-like [12,23], bag-like [13,24–29], and string-like models [30,31]. The problem of matching the Kerr–Newman exterior to an internal material source does not have a unique solution, because of the freedom in choosing the boundary between them [20].

The Kerr–Newman axially symmetric solution was obtained from the spherical Reissner–Nordström solution with help of the Newman–Janis algorithm [32].

As was shown by Gürses and Gürsey [33], the Newman–Janis algorithm belongs to the Trautman–Newman complex coordinate translations, and works for the algebraically special metrics of the Kerr–Schild class [34]. The spherical Kerr–Schild metrics written in

the units $c = G = 1$ and in the spacetime signature $[-+++]$, typical for the papers presented in the literature, have the form

$$ds^2 = -g(r)dt^2 + \frac{dr^2}{g(r)} + r^2d\Omega^2; \quad g(r) = 1 - \frac{2\mathcal{M}(r)}{r}; \quad \mathcal{M}(r) = 4\pi \int_0^r \rho(x)x^2dx \quad (4)$$

and present the algebraically degenerated solutions to the Einstein equations [33,34]. Stress–energy tensors for the spherical metrics (4) have the algebraic structure such that

$$T_t^t = T_r^r \quad (5)$$

where $T_t^t = \rho c^2$ is the density, and $T_t^t = -p_r$; $T_\theta^\theta = T_\phi^\phi = -p_\perp$ are the principal pressures. In the axially symmetric case, the condition (5) is not satisfied, while the relation $p_r = -\rho$ remains valid and characterizes the algebraic structure of stress–energy tensors for electromagnetic fields.

Most of the regular solutions presented in the literature for electrically charged rotating objects [35–45] belong to the Kerr–Schild class (for a review, see [46]).

An essential step in approaching electrically charged compact objects was presented by the nonlinear electrodynamics, developed by Born and Infeld and motivated by the aim to describe particles and the electromagnetic field in the frame of one physical entity which is the electromagnetic field [47]. The additional aim to avoid divergences of physical quantities remained inaccessible: the electromagnetic energy was made finite by imposing an upper cut-off on the electric field, although geometry remained singular (for the present status of the nonlinear electrodynamics [48–50]).

The Born–Infeld program can be realized in nonlinear electrodynamics minimally coupled to gravity, which describes regular electrically charged objects, related by electromagnetic and gravitational interactions, by the regular axially symmetric solutions, asymptotically Kerr–Newman for a distant observer, obtained from regular spherical solutions of the Kerr–Schild class specified by (5) [41,51,52]. Regular solutions of this class describe the regular rotating electrically charged black holes and electromagnetic spinning solitons, defined, following the Coleman definition for physical solitons [53], as non-singular non-dissipative particle-like structures without horizons, keeping themselves together by their own self-interaction.

Their basic features and typical behavior follow from general NED-GR equations which govern their behavior and, in the case of minimal coupling, do not involve any additional conditions concerning relations between electromagnetic and gravitational fields. The NED-GR dynamical equations describe these objects in the self-consistent way by the source-free equations for nonlinear electromagnetic fields, while their gravitational fields are determined by the Einstein equations with the source terms presented by the electromagnetic stress–energy tensors for their own electromagnetic fields.

The key point is the algebraic structure of the electromagnetic stress–energy tensors ($p_r = -\rho$). For regular solutions satisfying the weak energy condition (WEC), which requires non-negative energy density on any time-like curve, WEC inevitably leads to monotonic decreasing of density and to the existence of the de Sitter vacuum interiors, $p = -\rho$. This is the basic feature of all regular objects described by the metrics of the Kerr–Schild class, independently on a physical origin of a source term in the Einstein equations [54].

For spherical NED-GR objects, they are presented by the de Sitter center $r = 0$ [41]. For spinning objects, described by the axially symmetric geometry, the axial symmetry transforms the center $r = 0$ into the de Sitter equatorial disk $r = 0$, which is the obligatory constituent of all regular rotating objects [46,51,52]. In this paper, we show that WEC is always satisfied for regular rotating electrically charged NED-GR objects.

The mass of the objects with the de Sitter interiors is generically related to breaking of spacetime symmetry from the de Sitter group [55]. Intrinsic relation of the electromagnetic mass $m = 4\pi \int_0^\infty \rho_{em}r^2dr$ for NED-GR spinning solitons [56] with breaking of spacetime

symmetry [41], suggests the generic relation between spacetime symmetry and the Higgs mechanism, which supplies fermions with masses via spontaneous symmetry breaking of an incorporated scalar field from a false vacuum state $p = -\rho$ [57–59] (for a review, see [60,61]), due to intrinsic involvement of the de Sitter vacuum as its false vacuum state which leads to the direct relation of spontaneous symmetry breaking of the Higgs field with breaking of spacetime symmetry [54].

Regular rotating objects can, in principle, have two kinds of interiors, regulated by energy conditions [52,62]. The first type interior is represented by the de Sitter disk, the second type contains an additional closed de Sitter surface with the disk as a bridge. For NED-GR objects, the electromagnetic dynamics excludes the second type as incompatible with its standard requirement of non-negativity of the dielectric permeability [46,52].

The basic properties of electrically charged NED-GR spinning solitons have been verified by the observational case of appearance of a minimal length scale in the annihilation reaction $e^+e^- \rightarrow \gamma\gamma(\gamma)$. Experimental data, collected during fourteen years and worked out by the standard QED methods with the $O(\alpha^3)$ accuracy, revealed, with the 5σ significance, the existence of a characteristic minimal length scale $l_e = 1.57 \times 10^{-17}$ cm at $E = 1.253$ TeV [63,64]. The annihilation reaction $e^+e^- \rightarrow \gamma\gamma(\gamma)$ is purely electromagnetic and can be interpreted in the frame of the nonlinear electrodynamics minimally coupled to gravity. The NED-GR equations predict the existence of spinning electrically charged electromagnetic solitons, with the gyromagnetic ratio $g = 2$ for a distant observer. Basic model-independent features of electromagnetic spinning solitons visualizing annihilating particles provide a physical mechanism which can be responsible for appearance of a minimal length scale in annihilation, due to the balance between electromagnetic attraction of the oppositely charged annihilating particles and gravitational repulsion of their de Sitter vacuum interiors [64]. This case confirms the image of the electron as an extended spinning particle with the de Sitter vacuum interior, as suggested by the intrinsic involvement of the de Sitter vacuum in its electromagnetic mass.

Non-zero field components of the electromagnetic field tensor $F_{\alpha\beta}$, compatible with the axial symmetry, are $F_{01}, F_{02}, F_{13}, F_{23}$. Due to spacetime symmetry provided by the algebraic structure of electromagnetic stress–energy tensor, only two of them are independent and obey the system of four field equations. The necessary and sufficient condition for compatibility of this system has been obtained in our paper [52] and analyzed in [65]. In this paper, we study generic features of the Lagrange dynamics, obtain the general solution for the electromagnetic fields, show that all regular rotating electrically charged NED-GR objects satisfy the weak energy condition, and outline their basic generic properties.

In Section 2, we present the basic equations which govern the regular rotating electrically charged NED-GR objects. Section 3 is devoted to the analysis of the Lagrange dynamics. In Section 4, we present general solution to dynamical equations for electromagnetic fields, and outline the generic properties of electrically charged NED-GR objects as determined by the dynamical equations and by the compatibility condition. Section 5 contains conclusions.

2. Basic Equations

In this section, we introduce the basic equations describing geometry and electromagnetic fields of regular rotating electrically charged NED-GR objects, as determined by the spacetime symmetry and by the algebraic structure of the electromagnetic stress–energy tensor and analyze the weak energy condition.

2.1. Geometry

Spherically symmetric metrics of the Kerr–Schild class (4) have been transformed in the general model-independent way to the axially symmetric metrics in the frame of the Gürses–Gürsey formalism [33] (which includes the Newman–Janis algorithm [32]). In the Boyer–Lindquist coordinates r, θ, ϕ , related with the Cartesian coordinates by

$x^2 + y^2 = (r^2 + a^2) \sin^2 \theta$; $z = r \cos \theta$, the axially symmetric Gürses–Gürsey metric, written in the geometrical units $c = G = 1$, has the form [33]

$$ds^2 = \frac{2f - \Sigma}{\Sigma} dt^2 + \frac{\Sigma}{\Delta} dr^2 + \Sigma d\theta^2 - \frac{4af \sin^2 \theta}{\Sigma} dt d\phi + \left(r^2 + a^2 + \frac{2fa^2 \sin^2 \theta}{\Sigma} \right) \sin^2 \theta d\phi^2 \quad (6)$$

where the Lorentz signature is $[- + + +]$, and

$$\Sigma = r^2 + a^2 \cos^2 \theta; \quad \Delta = r^2 + a^2 - 2f(r); \quad f(r) = r\mathcal{M}(r). \quad (7)$$

The master function $f(r)$ asymptotically goes to $f(r) \rightarrow (mr - q^2/2)$ as $r \rightarrow \infty$, which represents the Kerr–Newman metric (1) for the exterior field of a rotating charged object as seen by a distant observer. The parameter m is the electromagnetic mass of an object, $m = 4\pi \int_0^\infty \rho(r)r^2 dr$, which originates from a related spherical solution. The parameter q is a constant of integration identified as an electric charge by the asymptotic Coulomb behavior in the weak field linear regime. In the Kerr–Newman geometry, the master function $f(r) = mr - q^2/2$ can change the sign which leads to causality violation [19]. In the regular geometry (6), the function $\mathcal{M}(r)$ monotonically grows from $\mathcal{M}(r) = 4\pi\rho(0)r^3/3 \rightarrow 0$ as $r \rightarrow 0$, to $\mathcal{M}(r) = m - q^2/2r \rightarrow m$ as $r \rightarrow \infty$ [41]. This guarantees the causal safety on the whole spacetime manifold due to $f(r) \geq 0$ [51].

In the axially symmetric geometry, the surfaces $r = \text{constant}$ are the confocal ellipsoids

$$r^4 - (x^2 + y^2 + z^2 - a^2)r^2 - a^2z^2 = 0 \quad (8)$$

which for $r = 0$ degenerate to the equatorial disk

$$x^2 + y^2 \leq a^2, \quad z = 0 \quad (9)$$

centered on the symmetry axis and confined by the ring [66]

$$x^2 + y^2 = a^2, \quad z = 0. \quad (10)$$

Spacetime horizons are defined by $\Delta(r) = r^2 + a^2 - 2r\mathcal{M}(r) = 0$ which gives

$$r_{+,-} = \mathcal{M}(r) \pm \sqrt{\mathcal{M}^2 - a^2}; \quad r_\pm = \mathcal{M}(r_\pm) \quad (11)$$

where r_+ is the event horizon, $r_- < r_+$ is the internal Cauchy horizon, and r_\pm is the double horizon for the extreme black hole with $a = a_{dh} = \mathcal{M}(r_\pm) = r_\pm$ [52,62].

Ergospheres as surfaces of the static limit $g_{tt} = 0$ confine ergoregions, where $g_{tt} < 0$ ensures extraction of rotational and electromagnetic energy ([45,46,52] and references therein).

The NED-GR black holes have one ergosphere for any density profile. For a spinning electromagnetic soliton, the existence of ergospheres depends on the density profile. They can have two ergospheres and ergoregions between them, or one ergosphere and the ergoregion involving the whole interior [52,62].

The anisotropic stress–energy tensor responsible for geometry (6) can be written as [33]

$$T_{\mu\nu} = (\rho + p_\perp)(u_\mu u_\nu - l_\mu l_\nu) + p_\perp g_{\mu\nu}; \quad (12)$$

$$u^\mu = \frac{1}{\sqrt{\pm\Delta\Sigma}} [(r^2 + a^2)\delta_0^\mu + a\delta_3^\mu], \quad l^\mu = \sqrt{\frac{\pm\Delta}{\Sigma}} \delta_1^\mu, \quad n^\mu = \frac{1}{\sqrt{\Sigma}} \delta_2^\mu, \quad m^\mu = \frac{-1}{\sqrt{\Sigma} \sin \theta} [a \sin^2 \theta \delta_0^\mu + \delta_3^\mu] \quad (13)$$

where the sign plus refers to the regions outside the event horizon and in the regular geometry inside the Cauchy horizon, where the vector u^μ is time-like. The vectors m^μ and n^μ are space-like in all regions. The eigenvalues of the stress–energy tensor (12) in the co-rotating reference frame, rotating with the angular velocity $\omega(r) = u^\phi / u^t = a / (r^2 + a^2)$, are defined by

$$T_{\mu\nu} u^\mu u^\nu = \rho(r, \theta); \quad T_{\mu\nu} l^\mu l^\nu = p_r = -\rho; \quad T_{\mu\nu} n^\mu n^\nu = T_{\mu\nu} m^\mu m^\nu = p_\perp(r, \theta). \quad (14)$$

In the regions outside the event horizon and inside the Cauchy horizon, where density is the eigenvalue of the time-like eigenvector u^μ , they are related to the function $f(r)$ as [27]

$$\rho(r, \theta) = \frac{r^4}{\Sigma^2} \tilde{\rho}(r) = \frac{2(f'r - f)}{\Sigma^2}; \quad p_\perp(r, \theta) = \left(\frac{r^4}{\Sigma^2} - \frac{2r^2}{\Sigma} \right) \tilde{\rho}(r) - \frac{r^3}{2\Sigma} \tilde{\rho}'(r) = \frac{2(f'r - f) - f''\Sigma}{\Sigma^2} \quad (15)$$

where $\tilde{\rho}(r)$ is the density profile and \tilde{p}_\perp is the transversal pressure for an original spherical solution. The prime denotes the derivative with respect to r .

In the equatorial plane, $\theta = \pi/2$, $(p_\perp + \rho) = -r\tilde{\rho}'(r)/2$ [51]. For the spherical solutions satisfying WEC, regularity requires $r\tilde{\rho}'(r) \rightarrow 0$ as $r \rightarrow 0$ [41]. As a result, on the disk (9) $p_\perp + \rho = 0 \rightarrow p_\perp = p_r = p = -\rho$, while the function $f(r)$ in (6) approaches the de Sitter asymptotic $2f(r) \rightarrow 8\pi G\tilde{\rho}(0)r^4/3$ [41], and the geometry and the equation of state on the disk

$$p = -\rho; \quad f(r) = \frac{r^4}{2r_0^2}; \quad r_0^2 = \frac{3}{8\pi G\tilde{\rho}(0)} \quad (16)$$

represent the rotating de Sitter vacuum in the co-rotating frame [51].

The interior de Sitter vacuum disk of the radius a is the basic generic feature of all regular rotating compact objects [51,52]. The mass parameter m appearing in the Kerr–Newman limit, $m = \mathcal{M}(r \rightarrow \infty)$, is the finite positive electromagnetic mass, generically related to the interior de Sitter vacuum and breaking of spacetime symmetry from the de Sitter group in its origin to the Poincaré group at infinity in the asymptotically flat spacetime [55,56]. For electromagnetic solitons, this leads to the inherent relation between gravity, spacetime symmetry, and the Higgs mechanism for mass generation [54,67]. The Higgs mechanism endows a particle with a mass via spontaneous symmetry breaking of an intrinsically incorporated scalar field from its false vacuum state $p = -\rho$ [57–59]. In this way, the Higgs mechanism generically incorporates the de Sitter vacuum $p = -\rho$ as its basic ingredient, in consequence, spontaneous symmetry breaking of a scalar field intrinsically involves breaking of spacetime symmetry from the de Sitter group [54].

2.2. Electromagnetic Fields

Non-zero field components, compatible with the axial symmetry, are $F_{01}, F_{02}, F_{13}, F_{23}$. In the spacetime geometry with the metric (6), they are related by

$$F_{31} = a \sin^2 \theta F_{10}; \quad aF_{23} = (r^2 + a^2)F_{02}. \quad (17)$$

The NED-GR dynamical equations are usually obtained with the action

$$\mathcal{I} = \frac{1}{16\pi G} \int d^4x \sqrt{-g} [R - \mathcal{L}(F)]; \quad F = F_{\mu\nu} F^{\mu\nu} \quad (18)$$

where R is the scalar curvature, and $F_{\mu\nu} = \partial_\mu A_\nu - \partial_\nu A_\mu$ is the electromagnetic tensor. The gauge-invariant electromagnetic Lagrangian $\mathcal{L}(F)$ should have the Maxwell limit in the weak field linear regime where its derivative $\mathcal{L}_F = d\mathcal{L}(F)/dF = 1$.

Variation with respect to A^μ in (18) and the contracted Bianchi identities $G^\mu_{\nu;\mu} = 0$, give two sets of the source-free dynamic field equations, respectively [39,51]

$$\nabla_\mu (\mathcal{L}_F F^{\mu\nu}) = 0; \quad (19)$$

$$\nabla_\mu {}^* F^{\mu\nu} = 0; \quad {}^* F^{\mu\nu} = \frac{1}{2} \eta^{\mu\nu\alpha\beta} F_{\alpha\beta}; \quad \eta^{0123} = -\frac{1}{\sqrt{-g}} \quad (20)$$

where g is the determinant of the metric tensor $g_{\mu\nu}$.

Introducing the field vectors

$$\mathbf{E} = \{F_{\beta 0}\}; \quad \mathbf{D} = \{\mathcal{L}_F F^{0\beta}\}; \quad \mathbf{B} = \{{}^* F^{\beta 0}\}; \quad \mathbf{H} = \{\mathcal{L}_F {}^* F_{0\beta}\},$$

we can write the field Equations (19) and (20) in the conventional form of the Maxwell equations

$$\nabla \cdot \mathbf{D} = 0; \quad \nabla \times \mathbf{H} = \partial \mathbf{D} / \partial t; \quad \nabla \cdot \mathbf{B} = 0; \quad \nabla \times \mathbf{E} = -\partial \mathbf{B} / \partial t. \tag{21}$$

The electric and magnetic induction \mathbf{D} and \mathbf{B} are related with the field strength \mathbf{E} and \mathbf{H} by $D^\alpha = \epsilon_\beta^\alpha E^\beta$; $B^\alpha = \mu_\beta^\alpha H^\beta$, where ϵ_α^β and μ_α^β are the dielectric and magnetic permeability.

Symmetry of spacetime (8) gives two independent eigenvalues [51]

$$\epsilon_r^r = \frac{(r^2 + a^2)}{\Delta} \mathcal{L}_F; \quad \epsilon_\theta^\theta = \mathcal{L}_F; \quad \mu_r^r = \frac{(r^2 + a^2)}{\Delta \mathcal{L}_F}; \quad \mu_\theta^\theta = \frac{1}{\mathcal{L}_F}. \tag{22}$$

For rotating regular objects, there exists a possibility of violation of the weak energy condition [43,44,52,65], which requires $\rho > 0$ and $p_\perp + \rho \geq 0$. The condition for testing WEC follows from (15) and has the form [52]

$$(p_\perp + \rho) = \frac{2r^2}{\Sigma^2} \left(\frac{\Sigma r}{4} |\rho'| - \bar{\rho} a^2 \cos^2 \theta \right) \tag{23}$$

which implies a possibility of generic violation of the weak energy condition.

In NED-GR, the regular rotating objects are presented by the electromagnetic stress–energy tensor, calculated in the standard way [68], which has the form [51]

$$T_\nu^\mu = 2\mathcal{L}_F F_{\nu\alpha} F^{\mu\alpha} - \frac{1}{2} \delta_\nu^\mu \mathcal{L} \tag{24}$$

and gives the source of the gravitational field in the Einstein equations $G_\nu^\mu = -8\pi G T_\nu^\mu$.

Let us note that in the axially symmetric spacetime, the condition (5) is not satisfied, because

$$T_0^0 = -\frac{2\mathcal{L}_F}{\Sigma} [(r^2 + a^2)F_{10}^2 + F_{20}^2] - \frac{\mathcal{L}}{2}; \quad T_1^1 = -2\mathcal{L}_F F_{10}^2 - \frac{\mathcal{L}}{2}. \tag{25}$$

In the spherical geometry $a = 0$, $\Sigma = r^2$ and $F_{20} = 0$, as a result the relations (25) give the relation (5) which specifies the spherical solutions of the Kerr–Schild class.

However, the equation of state $p_r = -\rho$ remains valid in the axially symmetric geometry. The electromagnetic density and pressures are defined by (14) as

$$\rho = \frac{1}{2} \mathcal{L} + 2\mathcal{L}_F F_{10}^2; \quad p_r = T_1^1 = -\rho; \quad p_\perp = -\frac{1}{2} \mathcal{L} + 2\mathcal{L}_F \frac{F_{20}^2}{a^2 \sin^2 \theta}. \tag{26}$$

For NED-GR objects, the basic equation for testing WEC follows directly from (26) as [51]

$$(p_\perp + \rho) = 2\mathcal{L}_F \left(F_{10}^2 + \frac{F_{20}^2}{a^2 \sin^2 \theta} \right). \tag{27}$$

Violation of the weak energy condition would require the negative values of the dielectric and magnetic permeability, according to (22). For NED-GR objects, the basic requirement of electrodynamics of continuous media (positivity of the dielectric permeability [68]) excludes WEC violation. It follows that for NED-GR objects, the weak energy condition is always satisfied. In the equatorial plane, $p_\perp + \rho = -r\rho'/2$ and WEC leads to a monotonic increase of electromagnetic density to its maximal value on the disk [51,52].

Spacetime of regular rotating electrically charged compact objects contains at most two horizons and one ergosphere for black holes, and one or two ergospheres for electromagnetic spinning solitons. Electromagnetic mass of an NED-GR object is generically related to breaking of spacetime symmetry

from the de Sitter group. The weak energy condition is satisfied for all regular electrically charged NED-GR compact objects.

3. Lagrange Dynamics

In this section, we analyze the general behavior of the field invariant F and the Lagrange derivatives \mathcal{L}_F and \mathcal{L}_{FF} , which determine the basic features of the Lagrange dynamics.

The general definition of a stress–energy tensor for the electromagnetic field (26) defines a general form of the Lagrangian as

$$\mathcal{L} = 2\rho - 4\mathcal{L}_F F_{10}^2. \tag{28}$$

On the disk, regularity requires $p_\perp + \rho = 0$, according to (16), and Equation (27) yields $F_{10}^2 = F_{20}^2/a^2 = 0$ since \mathcal{L}_F cannot be zero. Electromagnetic field components $F_{10} = 0, F_{20} = 0$, and consequently $F_{13} = 0, F_{23} = 0$, present the trivial solution to the dynamical Equations (19) and (20). On the disk where $F_{10} = 0$, the basic relation (28) gives

$$F_{10}^2 = \frac{2\rho - \mathcal{L}}{4\mathcal{L}_F} = 0. \tag{29}$$

For regular solutions with an arbitrary Lagrangian \mathcal{L} , it is possible if and only if $\mathcal{L}_F \rightarrow \infty$. The behavior of \mathcal{L}_F in the strong field regime on the disk represents the natural realization of the underlying hypothesis of nonlinearity replacing a singularity ([65] and references therein).

The field invariant is determined by two independent field components as

$$F = 2\left(\frac{F_{20}^2}{a^2 \sin^2 \theta} - F_{10}^2\right). \tag{30}$$

Generic features of the Lagrange dynamics are defined by general relations (27), (28) and (30). Expressing $F_{20}^2/a^2 \sin^2 \theta$ from (30) and F_{10}^2 from (28), we obtain

$$p_\perp + \rho = F\mathcal{L}_F + 2\rho - \mathcal{L}; \quad \nabla(p_\perp + \rho) = F\nabla\mathcal{L}_F + 2\nabla\rho. \tag{31}$$

As follows from (27), on the disk $F_{10}^2 = F_{20}^2 = 0$, and thus, $F = 0$ and $\nabla F = 0$. In the weak field limit at $r \rightarrow \infty$, where $(p_\perp + \rho) \rightarrow 0$ because $\rho \rightarrow 0$ for compact objects, the field invariant F takes zero value at infinity.

Near the disk $\nabla(p_\perp + \rho) > 0$ since $(p_\perp + \rho)$ grows from $(p_\perp + \rho) = 0$, $\nabla\mathcal{L}_F < 0$ since \mathcal{L}_F decreases from $\mathcal{L}_F \rightarrow \infty$, and $\nabla\rho < 0$ because ρ decreases from its maximal value, hence the field invariant must be negative to guarantee the proper behavior of $(p_\perp + \rho)$.

The field invariant F evolves from $F = -0$ in the strong nonlinear regime on the disk to $F = -0$ at infinity. Lagrangian $\mathcal{L}(F)$, as a function of the non-monotonic function F with equal limiting values, should suffer branching on a surface where the invariant F achieves its minimum [39,41].

It follows that the Lagrange dynamics for regular electrically charged structures is described by the non-uniform variational problem with the action [69]

$$\mathcal{I} = \mathcal{I}_{int} + \mathcal{I}_{ext} = \frac{1}{16\pi} \left[\int_{\Omega_{int}} (R - \mathcal{L}_{int}(F))\sqrt{-g}d^4x + \int_{\Omega_{ext}} (R - \mathcal{L}_{ext}(F))\sqrt{-g}d^4x \right]. \tag{32}$$

Each of the two parts of the manifold, Ω_{int} and Ω_{ext} , is confined by the space-like hypersurfaces $t = t_{in}$ and $t = t_{fin}$. The internal boundary between Ω_{int} and Ω_{ext} is defined as a time-like hypersurface Σ_c , at which the field invariant F achieves its minimum, and the external part Ω_{ext} is confined by the time-like 3-hypersurface at infinity, where electromagnetic fields vanish [69]. Variation in the action (32) yields the dynamical

equations (19) and (20) in both Ω_{int} and Ω_{ext} , and the standard boundary conditions on the surface Σ_c [69]

$$\int_{\Sigma_c} \left(\mathcal{L}_{F(int)} F_{\mu\nu(int)} - \mathcal{L}_{F(ext)} F_{\mu\nu(ext)} \right) \sqrt{-g} \delta A^\mu d\sigma^\nu = 0; \quad \mathcal{L}_{int} - 2\mathcal{L}_{F(int)} F_{int} = \mathcal{L}_{ext} - 2\mathcal{L}_{F(ext)} F_{ext}. \quad (33)$$

The Lagrangian given by the general formula (28), $\mathcal{L} = 2\rho - 4\mathcal{L}_F F_{10}^2$, behaves as $\mathcal{L} \rightarrow 2\tilde{\rho}(0)$ at approaching the disk, because $\mathcal{L}_F F_{10}^2 \rightarrow 0$ by virtue of (27). In the weak field limit when $\mathcal{L}_F \rightarrow 1$ and $F_{10} \rightarrow 0$ as $r \rightarrow \infty$, the Lagrangian is $\mathcal{L} = 2\rho \rightarrow 0$, since $\rho \rightarrow 0$ for compact objects with finite mass. The Lagrange derivative \mathcal{L}_F decreasing from $\mathcal{L}_F = \infty$ on the disk to $\mathcal{L}_F = 1$ in the weak field limit as $r \rightarrow \infty$, is finite in the branching surface, as follows from (27).

The behavior of the Lagrange derivative \mathcal{L}_{FF} is determined by $\nabla \mathcal{L}_F = \mathcal{L}_{FF} \nabla F$. At the branching surface, defined by $\nabla F = 0$, the derivative \mathcal{L}_{FF} breaks from $L_{FF} = \infty$ on an upper branch, where \mathcal{L}_F decreases from the infinite value on the disk and $\nabla \mathcal{L}_F < 0$, while the invariant F decreases to its minimum and $\nabla F < 0$, to $L_{FF} = -\infty$ on a lower branch, where \mathcal{L}_F still decreases and $\nabla \mathcal{L}_F < 0$, while the invariant F increases from its minimum and $\nabla F > 0$. On the upper branch, at approaching the disk, $\mathcal{L}_{FF} \rightarrow \infty$ due to $\nabla F \rightarrow 0$ and $\nabla \mathcal{L}_F > 0$ for $\mathcal{L}_F \rightarrow \infty$.

Hence, in the upper branch, L_{FF} evolves between two infinite values and should have a minimum somewhere in between. On the lower branch, L_{FF} evolves from $L_{FF} = -\infty$ at the branching surface to $L_{FF} = 0$ in the Maxwell weak field limit at $r \rightarrow \infty$.

The characteristic behavior in the Lagrange dynamics is shown in Figure 1 [69].

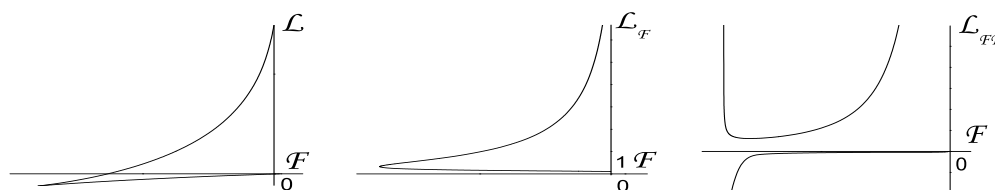


Figure 1. (Left) Typical behavior of the Lagrangian. (Middle) Behavior of the Lagrangian derivative \mathcal{L}_F . (Right) Characteristic behavior of the Lagrangian derivative \mathcal{L}_{FF} .

Generic behavior of the Lagrangian and its derivatives determines the basic features of the Lagrange dynamics. The field invariant evolves between two zero values, on the disk and at infinity, which leads to branching of the Lagrangian on the surface where the invariant F achieves its minimum. At the branching surface, the Lagrange derivative \mathcal{L}_{FF} breaks from $\mathcal{L}_{FF} \rightarrow \infty$ on the upper branch to $\mathcal{L}_{FF} \rightarrow -\infty$ on the lower branch.

4. General Solutions and Generic Properties of Regular Electrically Charged NED-GR Objects

In this section, we obtain the general solution and analyze the behavior of electromagnetic fields described by two independent components of the electromagnetic field tensor $F_{\mu\nu}$, which should satisfy the system of four dynamical equations and the necessary and sufficient condition for its compatibility. We also outline the basic properties of regular rotating electrically charged NED-GR objects.

4.1. General Solutions

The field Equations (19) and (20), with taking into account (17), form the system of four equations for two independent functions [52]

$$\frac{\partial}{\partial r} \left[(r^2 + a^2) \sin \theta \mathcal{L}_F F_{10} \right] + \frac{\partial}{\partial \theta} \left[\sin \theta \mathcal{L}_F F_{20} \right] = 0; \quad (34)$$

$$\frac{\partial}{\partial r} \left[a \sin \theta \mathcal{L}_F F_{10} \right] + \frac{\partial}{\partial \theta} \left[\frac{1}{a \sin \theta} \mathcal{L}_F F_{20} \right] = 0; \quad (35)$$

$$\frac{\partial}{\partial r} F_{20} - \frac{\partial}{\partial \theta} F_{10} = 0; \tag{36}$$

$$\frac{\partial}{\partial \theta} \left[a^2 \sin^2 \theta F_{10} \right] - \frac{\partial}{\partial r} \left[(r^2 + a^2) F_{20} \right] = 0. \tag{37}$$

In terms of the functions

$$U_{10} = \mathcal{L}_F F_{10}, \quad U_{20} = \mathcal{L}_F F_{20} \tag{38}$$

Equations (34) and (35) read

$$\frac{\partial}{\partial r} \left[(r^2 + a^2) \sin \theta U_{10} \right] + \frac{\partial}{\partial \theta} \left[\sin \theta U_{20} \right] = 0; \tag{39}$$

$$\sin \theta \frac{\partial}{\partial r} U_{10} = -\frac{1}{a^2} \frac{\partial}{\partial \theta} \left[\frac{1}{a \sin \theta} U_{20} \right] = 0 \tag{40}$$

and can be transformed to the form

$$U_{10} = \frac{1}{2a^2 r \sin \theta} \frac{\partial}{\partial \theta} \left(\frac{\Sigma}{\sin \theta} U_{20} \right); \tag{41}$$

$$\frac{\partial}{\partial \theta} \left\{ \frac{1}{\sin \theta} \left[\frac{\partial}{\partial r} \left(\frac{\Sigma}{r} U_{20} \right) + 2U_{20} \right] \right\} = 0. \tag{42}$$

Indeed, putting (40) into (39), we obtain the equation

$$U_{10} = \frac{(r^2 + a^2)}{2a^2 r \sin \theta} \frac{\partial}{\partial \theta} \left(\frac{1}{\sin \theta} U_{20} \right) - \frac{1}{2r \sin \theta} \frac{\partial}{\partial \theta} \left(\sin \theta U_{20} \right) = \frac{1}{2a^2 r \sin \theta} \frac{\partial}{\partial \theta} \left(\frac{\Sigma}{\sin \theta} U_{20} \right)$$

which evidently gives Equation (41). Putting then the function U_{10} , given by Equation (41), into Equation (40), we obtain Equation (42), which gives the first integral

$$\frac{\partial}{\partial r} \left(\frac{\Sigma}{r \sin \theta} U_{20} \right) + \frac{2U_{20}}{\sin \theta} = \Phi(r) \tag{43}$$

where the integration function $\Phi(r)$ is an arbitrary function of r . Introducing the function

$$V_{20} = \frac{\Sigma}{r \sin \theta} U_{20}, \tag{44}$$

we transform Equation (43) to

$$\frac{\partial}{\partial r} V_{20} + \frac{2r}{\Sigma} V_{20} = \Phi(r) \tag{45}$$

which has the form $y' + p(r)y = \Phi(r)$ with $p(r) = 2r/\Sigma$. Its general solution is

$$y(r) = \exp\left(-\int p(r)dr\right) \int f(r) \exp\left(\int p(r)dr\right)dr + A \exp\left(-\int p(r)dr\right)$$

which gives

$$V_{20}(r, \theta) = \Sigma^{-1} \int \Phi(r) \Sigma dr + \Psi_0(\theta) \Sigma^{-1}.$$

As a result, the general solution for the field function U_{20} is given by

$$U_{20}(r, \theta) = \frac{r}{\Sigma^2} \left[\Psi(\theta) + \sin \theta \int \Phi(r) \Sigma(r, \theta) dr \right], \tag{46}$$

where the integration function $\Psi(\theta)$ is an arbitrary function of θ .

The general solution for U_{10} follows from the relation (41) as

$$U_{10}(r, \theta) = \frac{1}{2a^2 \sin^3 \theta \Sigma^2} \left[\Sigma \Psi'(\theta) \sin \theta - [\Sigma - 2a^2 \sin^2 \theta] \Psi(\theta) \cos \theta \right] + \frac{\cos \theta}{\Sigma^2} \left[\int \Phi(r) r^2 dr - r^2 \int \Phi(r) dr \right]. \tag{47}$$

Formulae (46) and (47) present the general solution to the system (39) and (40), and thus to the system (34) and (35). Now, we consider Equations (36) and (37) to obtain conditions which should be satisfied by the integration functions $\Phi(r)$ and $\Psi(\theta)$, as the conditions required for the solution (46) and (47) to present a general solution to the whole dynamical system (34) and (37).

Equation (37) can be transformed as

$$F_{10} = \frac{1}{a^2 \sin 2\theta} \frac{\partial}{\partial r} \left[(r^2 + a^2) F_{20} \right] - \frac{\sin^2 \theta}{\sin 2\theta} \frac{\partial}{\partial \theta} F_{10} = \frac{1}{a^2 \sin 2\theta} \frac{\partial}{\partial r} \left[(r^2 + a^2 - a^2 \sin^2 \theta) F_{20} \right] + \frac{\sin^2 \theta}{\sin 2\theta} \frac{\partial F_{20}}{\partial r} - \frac{\sin^2 \theta}{\sin 2\theta} \frac{\partial F_{10}}{\partial \theta} = \frac{1}{a^2 \sin 2\theta} \frac{\partial}{\partial r} \left(\Sigma F_{20} \right) - \frac{\sin^2 \theta}{\sin 2\theta} \left[\frac{\partial F_{20}}{\partial r} - \frac{\partial F_{10}}{\partial \theta} \right]$$

and gives, along with the Equation (36), the system

$$\frac{\partial F_{10}}{\partial \theta} - \frac{\partial F_{20}}{\partial r} = 0; \quad F_{10} = \frac{1}{a^2 \sin 2\theta} \frac{\partial}{\partial r} \left(\Sigma F_{20} \right). \tag{48}$$

To the first equation of system (48), we put F_{10} from the second equation, which transforms the first equation to the form

$$\frac{\partial}{\partial \theta} \left[\frac{1}{a^2 \sin 2\theta} \frac{\partial}{\partial r} \left(\Sigma F_{20} \right) \right] - \frac{\partial F_{20}}{\partial r} = 0.$$

As a result, the system of Equations (36) and (37) takes the form

$$F_{10} = \frac{1}{a^2 \sin 2\theta} \frac{\partial}{\partial r} \left(\Sigma F_{20} \right); \tag{49}$$

$$\frac{\partial}{\partial r} \left\{ \frac{\partial}{\partial \theta} \left(\frac{\Sigma}{\sin 2\theta} F_{20} \right) - a^2 F_{20} \right\} = 0. \tag{50}$$

In terms of the function U_{10} , Equation (49) reads

$$U_{10} = \frac{\mathcal{L}_F}{a^2 \sin 2\theta} \frac{\partial}{\partial r} \left(\frac{\Sigma}{\mathcal{L}_F} U_{20} \right). \tag{51}$$

On the other hand, the function U_{10} should satisfy Equation (41). Equality of both these expressions gives the first constraint which should be satisfied by the function U_{20} as the general solution to the system (41) and (42)

$$r \frac{\partial}{\partial r} \left(\Sigma U_{20} \right) - \cos \theta \frac{\partial}{\partial \theta} \left(\frac{\Sigma}{\sin \theta} U_{20} \right) = \mathcal{B}(\mathcal{L}_F); \tag{52}$$

$$\mathcal{B}(\mathcal{L}_F) = \frac{r}{\mathcal{L}_F} \frac{\partial \mathcal{L}_F}{\partial r} \Sigma U_{20}. \tag{53}$$

Now, let us consider Equation (50). Writing it for U_{20} , and taking into account that the function U_{20} should satisfy Equation (42), we obtain the second constraint for U_{20}

$$\frac{\partial}{\partial r} \left\{ \frac{\partial}{\partial \theta} \left(\frac{\Sigma}{\sin 2\theta} U_{20} \right) - a^2 U_{20} \right\} = \mathcal{A}(\mathcal{L}_F); \tag{54}$$

$$\begin{aligned} \mathcal{A}(\mathcal{L}_F) &= \frac{1}{\mathcal{L}_F} \frac{\partial \mathcal{L}_F}{\partial r} \frac{\partial}{\partial \theta} \left(\frac{\Sigma}{\sin 2\theta} U_{20} \right) + \frac{1}{\mathcal{L}_F} \frac{\partial \mathcal{L}_F}{\partial \theta} \frac{\partial}{\partial r} \left(\frac{\Sigma}{\sin 2\theta} U_{20} \right) \\ &+ \mathcal{L}_F \frac{\partial}{\partial r} \left(\frac{1}{\mathcal{L}_F^2} \frac{\partial \mathcal{L}_F}{\partial \theta} \right) \frac{\Sigma}{\sin 2\theta} U_{20} - \frac{a^2}{\mathcal{L}_F} \frac{\partial \mathcal{L}_F}{\partial r} U_{20}. \end{aligned} \tag{55}$$

We have two equations, (52) and (54), which should be satisfied by the function U_{20} , while the function U_{10} can be found from relation (41) either (51). It follows that the two constraints (52) and (54) should be satisfied by the integration functions $\Phi(r)$, $\Psi(\theta)$ and serve for their specification in general solutions for U_{20} and U_{10} and, thus, for the field functions F_{20} and F_{10} .

Putting relation (46) into (52) and taking into account (53), we present the first constraint (52) as the integro-differential equation for the integration functions $\Phi(r)$ and $\Psi(\theta)$

$$\begin{aligned} &\Psi'(\theta) + (\tan \theta - \cot \theta) \Psi(\theta) - \sin \theta \tan \theta r \Sigma \Phi(r) \\ &+ \sin \theta \tan \theta \int \Phi(r) r^2 dr - a^2 \sin^2 \theta \cos \theta \int \Phi(r) dr \\ &= -\frac{\Sigma \sin \theta}{r \cos \theta} \mathcal{B}(\mathcal{L}_F) = -\frac{r \tan \theta}{\mathcal{L}_F} \frac{\partial \mathcal{L}_F}{\partial r} \left[\Psi(\theta) + \sin \theta \int \Phi(r) \Sigma(r, \theta) dr \right]. \end{aligned} \tag{56}$$

Now, we transform the second constraint (54) by replacing the derivative with respect to θ from the first constraint (52), which yields, after simple algebra,

$$\frac{\partial}{\partial r} \left[r \frac{\partial}{\partial r} (\Sigma U_{20}) + (r^2 - a^2 \cos^2 \theta) U_{20} \right] = 2 \cos^2 \theta \mathcal{A}(\mathcal{L}_F) + \frac{\partial}{\partial r} \mathcal{B}(\mathcal{L}_F). \tag{57}$$

Taking into account Equation (43) gives

$$r \frac{\partial}{\partial r} (\Sigma U_{20}) = r^2 \Phi(r) \sin \theta + (a^2 \cos^2 \theta - r^2) U_{20}$$

and reduces the second constraint on the integration functions to the form

$$\sin \theta \frac{\partial}{\partial r} (r^2 \Phi(r)) = 2 \mathcal{A}(\mathcal{L}_F) \cos^2 \theta + \frac{\partial}{\partial r} \mathcal{B}(\mathcal{L}_F). \tag{58}$$

Applying the expressions (53) and (55) in the right-hand side of Equation (58), we obtain the second constraint dependent on the general solution U_{20}

$$\begin{aligned} \sin \theta \frac{\partial}{\partial r} (r^2 \Phi(r)) &= \frac{\cot \theta}{\mathcal{L}_F} \frac{\partial \mathcal{L}_F}{\partial r} \frac{\partial}{\partial \theta} (\Sigma U_{20}) + \left[\frac{r}{\mathcal{L}_F} \frac{\partial \mathcal{L}_F}{\partial r} + \frac{\cot \theta}{\mathcal{L}_F} \frac{\partial \mathcal{L}_F}{\partial \theta} \right] \frac{\partial}{\partial r} (\Sigma U_{20}) \\ &+ \frac{1}{\mathcal{L}_F \Sigma} \frac{\partial \mathcal{L}_F}{\partial r} (r^2 - a^2 \cos^2 \theta) \Sigma U_{20} + \frac{1}{\mathcal{L}_F} \frac{\partial \mathcal{L}_F}{\partial r} (1 - \cot^2 \theta) \Sigma U_{20} \\ &+ \left[\frac{\cot \theta}{\mathcal{L}_F} \left(\frac{\partial}{\partial r} \frac{\partial \mathcal{L}_F}{\partial \theta} - \frac{2}{\mathcal{L}_F} \frac{\partial \mathcal{L}_F}{\partial r} \frac{\partial \mathcal{L}_F}{\partial \theta} \right) + \frac{r}{\mathcal{L}_F} \left(\frac{\partial}{\partial r} \frac{\partial \mathcal{L}_F}{\partial r} - \frac{1}{\mathcal{L}_F} \left(\frac{\partial \mathcal{L}_F}{\partial r} \right)^2 \right) \right] \Sigma U_{20}. \end{aligned} \tag{59}$$

Then, we express the derivatives of ΣU_{20} via the integration functions in (46), which gives

$$\frac{\partial}{\partial \theta} (\Sigma U_{20}) = \frac{r}{\Sigma^2} \left[\Sigma \Psi'(\theta) + a^2 \sin 2\theta \Psi(\theta) - a^2 \Sigma \sin \theta \sin 2\theta \int \Phi(r) dr \right]$$

$$+ \frac{r \cos \theta}{\Sigma^2} (2a^2 \sin^2 \theta + \Sigma) \int \Phi(r) \Sigma(r, \theta) dr; \tag{60}$$

$$\frac{\partial}{\partial r} (\Sigma U_{20}) = r \sin \theta \Phi(r) + \frac{(a^2 \cos^2 \theta - r^2)}{\Sigma^2} \left[\Psi(\theta) + \sin \theta \int \Phi(r) \Sigma(r, \theta) dr \right]. \tag{61}$$

Finally, putting these expressions and the general solution (46) into Equation (58), we obtain, after collecting similar terms, the second constraint on the integration functions

$$\sin \theta \frac{d}{dr} (r^2 \Phi(r)) = D_1 \Phi(r) + D_2 \left[\Psi'(\theta) - a^2 \sin \theta \sin 2\theta \int \Phi(r) dr \right] + D_3 \Psi(\theta) + D_4 \int \Phi(r) \Sigma(r, \theta) dr \tag{62}$$

$$D_1 = \frac{r \sin \theta (a^2 \cos^2 \theta - r^2)}{\mathcal{L}_F \Sigma^2} \left[r \frac{\partial \mathcal{L}_F}{\partial r} + \cot \theta \frac{\partial \mathcal{L}_F}{\partial \theta} \right]; \quad D_2 = \frac{r \cot \theta \partial \mathcal{L}_F}{\mathcal{L}_F \Sigma \partial r}; \tag{63}$$

$$D_3 = \frac{1}{\mathcal{L}_F} \frac{\partial \mathcal{L}_F}{\partial r} \frac{r}{\Sigma^2 \sin^2 \theta} (2a^2 \cos^2 \theta \sin^2 \theta - \Sigma \cos 2\theta) + \frac{\cot \theta \partial \mathcal{L}_F}{\mathcal{L}_F \partial \theta} \frac{(a^2 \cos^2 \theta - r^2)}{\Sigma^2} + \frac{r}{\mathcal{L}_F \Sigma} \left[\cot \theta \left(\frac{\partial}{\partial r} \frac{\partial \mathcal{L}_F}{\partial \theta} - \frac{2}{\mathcal{L}_F} \frac{\partial \mathcal{L}_F}{\partial r} \frac{\partial \mathcal{L}_F}{\partial \theta} \right) + r \left(\frac{\partial}{\partial r} \frac{\partial \mathcal{L}_F}{\partial r} - \frac{1}{\mathcal{L}_F} \left(\frac{\partial \mathcal{L}_F}{\partial r} \right)^2 \right) \right]; \tag{64}$$

$$D_4 = \frac{r}{\mathcal{L}_F \Sigma^2} \frac{\partial \mathcal{L}_F}{\partial r} (\Sigma + 2a^2 \cos^2 \theta) \sin \theta + \frac{\cot \theta \partial \mathcal{L}_F}{\mathcal{L}_F \partial \theta} \frac{(a^2 \cos^2 \theta - r^2) \sin \theta}{\Sigma^2} + \frac{r \sin \theta}{\mathcal{L}_F \Sigma} \left[\cot \theta \left(\frac{\partial}{\partial r} \frac{\partial \mathcal{L}_F}{\partial \theta} - \frac{2}{\mathcal{L}_F} \frac{\partial \mathcal{L}_F}{\partial r} \frac{\partial \mathcal{L}_F}{\partial \theta} \right) + r \left(\frac{\partial}{\partial r} \frac{\partial \mathcal{L}_F}{\partial r} - \frac{r}{\mathcal{L}_F} \left(\frac{\partial \mathcal{L}_F}{\partial r} \right)^2 \right) \right]. \tag{65}$$

Let us summarize the obtained result:

The general solution for the field components is given by

$$F_{20}(r, \theta) = \frac{r}{\mathcal{L}_F \Sigma^2} \left[\Psi(\theta) + \sin \theta \int \Phi(r) \Sigma(r, \theta) dr \right]; \tag{66}$$

$$F_{10}(r, \theta) = \frac{1}{2a^2 \sin^3 \theta \mathcal{L}_F \Sigma^2} \left[\sin \theta \Sigma \Psi'(\theta) - \cos \theta [\Sigma - 2a^2 \sin^2 \theta] \Psi(\theta) \right] + \frac{\cos \theta}{\mathcal{L}_F \Sigma^2} \left[\int \Phi(r) r^2 dr - r^2 \int \Phi(r) dr \right]. \tag{67}$$

The integration functions $\Phi(r)$ and $\Psi(\theta)$ are specified by the basic conditions (56) and (62). In addition, the Lagrange derivative \mathcal{L}_F should satisfy the necessary and sufficient condition of compatibility of the system of four Equations (34)–(37), and hence (19) and (20), for the two independent functions F_{10} and F_{20} , which read [52]

$$\frac{\partial}{\partial r} \left(\frac{1}{\mathcal{L}_F} \frac{\partial \mathcal{L}_F}{\partial \theta} \right) \frac{\partial}{\partial \theta} \left(\frac{1}{\mathcal{L}_F} \frac{\partial \mathcal{L}_F}{\partial r} \right) + \frac{4a^2 \sin^2 \theta}{\Sigma^2} \frac{1}{\mathcal{L}_F^2} \left[r \frac{\partial \mathcal{L}_F}{\partial r} + \cot \theta \frac{\partial \mathcal{L}_F}{\partial \theta} \right]^2 = 0. \tag{68}$$

This condition is evidently satisfied for $\mathcal{L}_F = const$, which can be normalized to $\mathcal{L}_F = 1$ corresponding to the Maxwell weak field limit, and in the case of trivial zero field solutions $F_{10} = F_{20} = 0$ [52]. In the weak field limit $\mathcal{L}_F = 1$, integration of Equation (58) gives the integration function $\Phi(r)$ as

$$\Phi(r) = \frac{C_1}{r^2}.$$

Putting it into Equation (56), we obtain the equation for a second integration function

$$\Psi' + (\tan \theta - \cot \theta) \Psi = 0$$

whose solution is given by

$$\Psi(\theta) = C_2 \sin 2\theta$$

where C_1 and C_2 are the arbitrary integration constants, and solutions for F_{10} and F_{20} in the Maxwell weak field linear limit $\mathcal{L}_F = 1$ are given by

$$F_{10} = C_1 \frac{2r \cos \theta}{\Sigma^2} + C_2 \frac{(a^2 \cos^2 \theta - r^2)}{a^2 \Sigma^2}; \quad F_{20} = C_1 \frac{\sin \theta (r^2 - a^2 \cos^2 \theta)}{\Sigma^2} + C_2 \frac{r \sin 2\theta}{\Sigma^2}. \quad (69)$$

Choosing the integration constants $C_1 = 0$, $C_2 = -qa^2$, we reduce the integration functions to

$$\Phi(r) = 0; \quad \Psi(\theta) = -qa^2 \sin 2\theta. \quad (70)$$

Applying them in the relations (66) and (67), we obtain the solution

$$F_{01} = -\frac{q(r^2 - a^2 \cos^2 \theta)}{\Sigma^2 \mathcal{L}_F}; \quad F_{02} = \frac{qa^2 r \sin 2\theta}{\Sigma^2 \mathcal{L}_F}; \quad F_{31} = a \sin^2 \theta F_{10}; \quad aF_{23} = (r^2 + a^2)F_{02} \quad (71)$$

which satisfies the dynamical Equations (34)–(37) and thus (19) and (20), gives the known solution [19,25] in the Maxwell limit $\mathcal{L}_F = 1$, and satisfies the compatibility condition (68) on the disk due to $\mathcal{L}_F \Sigma^2 \rightarrow \infty$ and $\mathcal{L}_F \rightarrow \infty$ [52].

Indeed, introducing solutions (71) to (27), we obtain the basic relations

$$(p_{\perp} + \rho) = \frac{2q^2}{\mathcal{L}_F \Sigma^2}; \quad F = -\frac{(p_{\perp} + \rho)^2 \Sigma^2}{2q^2}. \quad (72)$$

It follows that at approaching the disk, $(\mathcal{L}_F \Sigma^2)^{-1} \rightarrow (p_{\perp} + \rho)$ and $F \rightarrow -0$, which ensures regularity of the solution. At the same time, the behavior of $(\mathcal{L}_F \Sigma^2) \rightarrow \infty$ as $(p_{\perp} + \rho)^{-1}$, and $\mathcal{L}_F \rightarrow \infty$ as $(p_{\perp} + \rho)^{-1} \Sigma^{-2}$, provides satisfaction of the compatibility condition (68) on the disk, where $(p_{\perp} + \rho) = 0$ and $\Sigma = 0$.

4.2. Generic Behavior of Electrically Charged NED-GR Objects

The basic generic feature of all regular rotating electrically charged NED-GR objects is the interior de Sitter vacuum disk, $p = -\rho$. All these objects satisfy the weak energy condition; as a result, the electromagnetic density achieves its maximal value on the disk, where electromagnetic field vanishes, so that the maximal density represents the density of electromagnetic vacuum with the de Sitter equation of state $p = -\rho$ [41].

Regularity requires $\mathcal{L}_F \rightarrow \infty$ on the disk. In accordance with the general relation (22), in the strongly nonlinear regime on the disk, the magnetic permeability $\mu_r^r = \mu_{\theta}^{\theta} = \mu = 1/\mathcal{L}_F$ vanishes, the dielectric permeability $\epsilon_r^r = \epsilon_{\theta}^{\theta} = \mathcal{L}_F$ tends to infinity, and the disk (9) represents the perfect conductor and ideal diamagnet [51].

Applying the solution (71) which satisfies the dynamical system (19) and (20) and the compatibility condition (68) on the disk, we calculate the surface current, $4\pi j_k = [e_{(k)}^{\alpha} F_{\alpha\beta} n^{\beta}]$, where $e_{(k)}^{\alpha}$ are the base vectors related to the coordinates on the disk $t, \phi, 0 \leq \xi \leq \pi/2$; the vector $n_{\alpha} = \delta_{\alpha}^1 (1 + q^2/a^2)^{-1/2} \cos \xi$ is the unit normal to the disk, and $[..]$ denotes a jump across the disk in the direction orthogonal to it [20]. This gives [70]

$$j_{\phi} = -\frac{qc}{2\pi a} \sqrt{1 + q^2/a^2} \sin^2 \xi \frac{\mu}{\cos^3 \xi}. \quad (73)$$

On the disk, the magnetic permeability vanishes, $\mu = 1/\mathcal{L}_F = 0$; as a result, the surface current j_{ϕ} is zero over the disk—except the ring $\xi = \pi/2$, where both terms in the second fraction zero out independently. As a result, the current can have any non-zero value, and satisfies the general criterion for a superconducting current [68]. The superconducting current flows without resistance within the perfect conductor, and represents thus a non-dissipative source of the electromagnetic field, which provides practically unlimited lifetime of an object [70].

The circular current (73) produces a magnetic momentum μ_{in} which is *intrinsic* in principle, because the dynamical Equations (19) and (20) are source-free [71]. At approaching the disk (9), $r \rightarrow 0$ and the function $f(r)$ in (6) tends to zero, the disk is intrinsically flat [51] and the magnetic momentum is defined as $\mu_{in} = c^{-1}j_\phi S$, where S is the disk area. Expressing the current (73) in the form $j_\phi = -(qc/2\pi a) \sqrt{1+q^2/a^2}U$, where U is an uncertain coefficient, we rewrite the magnetic momentum as $\mu_{in} = -(qS/2\pi a) \sqrt{1+q^2/a^2}U$. When the intrinsic magnetic moment of an object is known, the uncertain coefficient U can be restored from μ_{in} . For an electromagnetic soliton with the parameters of the electron, this gives $j_\phi = 79.277$ A as the current which powers the electron for a practically unlimited lifetime [71].

For a distant observer, $r \gg \lambda_e = \hbar/m_e c$, the electric and magnetic field of the electromagnetic soliton with the parameters of the electron is given by [70]

$$E_r = -\frac{e}{r^2} \left(1 - \frac{\hbar^2}{m_e^2 c^2} \frac{3 \cos^2 \theta}{4r^2} \right); \quad E_\theta = \frac{e\hbar^2}{m_e^2 c^2} \frac{\sin 2\theta}{4r^3}. \tag{74}$$

$$B^r = -\frac{e\hbar}{m_e c} \frac{\cos \theta}{r^3} = 2\mu_e \frac{\cos \theta}{r^3}; \quad B_\theta = -\mu_e \frac{\sin \theta}{r^4}. \tag{75}$$

where $\lambda_e = \hbar/m_e c$ is the Compton wavelength of the electron. These expressions follow from the regular solutions [52,70] in the Kerr–Newman limit $r \gg \lambda_e = \hbar/m_e c$, and concord with Carter’s discovery of the ability of the Kerr–Newman metric to represent the electron as seen by a distant observer [19]. The leading term in E_r presents the Coulomb law as the classical limit $\hbar = 0$, while the higher terms give the quantum corrections.

An NED-GR image of the electron as an extended spinning particle has been confronted with the observational case presented by the purely electromagnetic annihilation reaction $e^+e^- \rightarrow \gamma\gamma(\gamma)$, which can shed some light on the electron internal structure. Analysis of the the most extensive available data set on the annihilation reaction $e^+e^- \rightarrow \gamma\gamma(\gamma)$, collected between 1989 and 2003 at energies from $\sqrt{s}=55$ GeV to 207 GeV, where \sqrt{s} is the center-of-mass energy, revealed, with the 5σ significance, the existence of the limit on the maximal resolution, shown in Figure 2, at the energy $E = 1.253$ TeV and the limiting length scale $l_e \simeq 1.57 \times 10^{-17}$ cm [63,64].

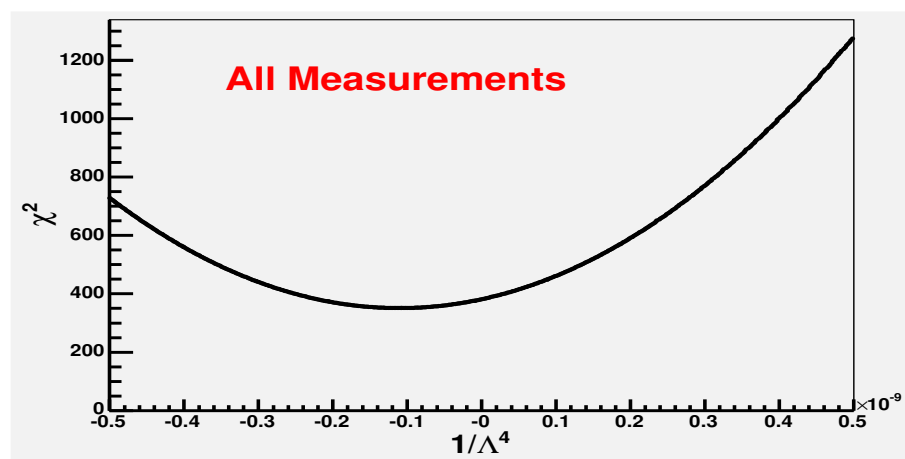


Figure 2. The minimum in the χ^2 fit with $P = 1/\Lambda^4$ where Λ is the QED cutoff parameter.

In Quantum Electrodynamics (QED), an electron is postulated as a point and the question of its internal structure is not addressed. Such an assumption works perfectly well, due to the technique invented by Richard Feynman, in the analysis of processes in which experimental distances are much bigger than a characteristic size of a particle.

Analysis of data on the reaction $e^+e^- \rightarrow \gamma\gamma(\gamma)$ in the QED- α^3 with assuming a scattering center as a point and calculating the radiative corrections up to $O(\alpha^3)$, predicted the increase of

the total cross-section. Contrary to the QED prediction, the χ^2 fit, shown in Figure 2, displayed the minimum with the negative fit parameter $P = (1/\Lambda^4)_{best} = -(4.05 \pm 0.73) \times 10^{-13} \text{GeV}^{-4}$, where Λ is the QED cutoff parameter [63,64]. The contradiction between the experimental results and the QED prediction testifies for a non-point-like behavior of particles in the physical situation when characteristic sizes of particles exceed the test distances. In the case of the electron, both its classical radius $r_e = e^2/(m_e c^2) = 2.8 \times 10^{-13} \text{cm}$ and the Compton size $\lambda_e = \hbar/(m_e c) = 3.9 \times 10^{-11} \text{cm}$ are much larger than the characteristic test length $l_e \simeq 1.57 \times 10^{-17} \text{cm}$.

The definite feature of the annihilation process is that at its final stage, a region of interaction is neutral and spinless. For any regular structure with the de Sitter interior, there exists the characteristic surface of zero gravity $r_* \simeq (r_0^2 r_g)^{1/3}$, at which the strong energy condition ($\rho + \sum p_k \geq 0$ [72]) is violated, the gravitational acceleration changes the sign and becomes repulsive [55,73]. The gravitational radius r_g , related to the energy $E = 1.253 \text{TeV}$, and de Sitter radius r_0 , related to the Higgs vacuum expectation value responsible for the electron mass at the scale $E_{EW} = 246 \text{GeV}$, give $r_* \simeq 0.86 \times 10^{-16} \text{cm}$. The test scale $l_e = 1.57 \times 10^{-17} \text{cm}$ appears inside a region with the repulsive gravity and can be understood as a distance of the closest approach of annihilating particles, at which their electromagnetic attraction is balanced by the gravitational repulsion of their interior de Sitter vacuum [10,64].

Remarkably, the appearance of the minimal length scale in the annihilation reaction $e^+e^- \rightarrow \gamma\gamma(\gamma)$ can be explained by the intrinsically negative pressure of the de Sitter vacuum, which is responsible, at other energy scales, for the accelerated expansion of our universe in the first inflation and today [74–81].

The general solution for two independent field components governed by the system of four dynamical equations should satisfy the condition of its compatibility and two conditions on two integration functions, which determine the basic properties and generic behavior of regular rotating electrically charged NED-GR objects, including the physical origin of their electromagnetic fields and of intrinsic magnetic momenta, and the minimal length scale in the annihilation reaction $e^+e^- \rightarrow \gamma\gamma(\gamma)$.

5. Conclusions

Generic behavior of electromagnetic fields for regular rotating electrically charged NED-GR objects is determined in a self-consistent and model-independent way, by spacetime symmetry related to the algebraic structure of electromagnetic stress–energy tensors ($p_r = -\rho$). Electromagnetic fields are described by source-free nonlinear equations, while the stress–energy tensor of these electromagnetic fields generates a gravitational field as a source term in the Einstein equations. Dynamical equations for electromagnetic fields form the system of four equations for two independent components of the electromagnetic tensor $F_{\mu\nu}$, due to spacetime symmetry. The Lagrange derivative \mathcal{L}_F is constrained by the compatibility condition for this system, while general solutions for field components are constrained by two conditions imposed on their originally arbitrary integration functions.

The fundamental generic feature of all regular rotating electrically charged NED-GR objects, uniquely determined by spacetime symmetry provided by the algebraic structure of the electromagnetic stress–energy tensor, is the existence of the interior disk of the de Sitter vacuum, which prevents a formation of a singularity by its intrinsic negative pressure (for a review, see [82]).

Electromagnetic mass of a regular electrically charged NED-GR object, $m = 4\pi \int_0^\infty \rho_{em} r^2 dr$, is generically related with gravity and breaking of the spacetime symmetry from the de Sitter group, which is the basic generic property of all regular objects involving an interior de Sitter vacuum [55].

All regular rotating electrically charged NED-GR objects satisfy the weak energy condition.

On the interior de Sitter vacuum disk, the magnetic permeability vanishes while the dielectric permeability goes to infinity; as a result, the de Sitter disk displays the properties of a perfect conductor and an ideal diamagnetic.

The ring confining the de Sitter vacuum disk comprises the superconducting current which powers the nonlinear electromagnetic field of an electrically charged NED-GR compact object and provides, as the non-dissipative source, its in principle unlimited lifetime, as well as the physical origin for its intrinsic magnetic momentum. For the electron visualized as the electromagnetic spinning soliton, this superconducting current is evaluated as $j_\phi = 79.277$ A [71].

NED-GR predicts, without any additional assumptions and constraints, the existence of electromagnetic spinning solitons (compact objects made of nonlinear electromagnetic field and bound by their electromagnetic and gravitational self-interaction), in agreement with the prominent proposal of Born and Infeld [47] to describe particles and the electromagnetic field in the frame of one physical entity (electromagnetic field).

The image of the electron as an extended particle, verified by application of an electromagnetic spinning soliton with the parameters of the electron for interpretation of experimental data on the purely electromagnetic annihilation reaction $e^+e^- \rightarrow \gamma\gamma(\gamma)$, allows to provide a certain physical explanation for appearance of the minimal length scale in the annihilation reaction $e^+e^- \rightarrow \gamma\gamma(\gamma)$.

Author Contributions: Authors contributed equally to this work. All authors have read and agreed to the published version of the manuscript.

Funding: This research received no external funding.

Data Availability Statement: Data supporting reported results can be found in [63,64].

Conflicts of Interest: The authors declare no conflict of interest.

References

- Wald, R.M. Black hole in a uniform magnetic field. *Phys. Rev. D* **1974**, *10*, 1680–1685. [CrossRef]
- Kovar, J.; Slany, P.; Cremaschini, C.; Stuchlik, Z. Electrically charged matter in rigid rotation around magnetized black hole. *Phys. Rev. D* **2014**, *90*, 044029. [CrossRef]
- Hamilton, A.J.S. Interior structure of rotating black holes. III. Charged black holes. *Phys. Rev. D* **2011**, *84*, 124057. [CrossRef]
- Crispino, L.C.B.; Dolan, S.R.; Higushi, A.; de Oliveira, E.S. Inferring black hole charge from backscattered electromagnetic radiation. *Phys. Rev. D* **2014**, *90*, 064027. [CrossRef]
- Abraham, M. Prinzipien der dynamik des electrons. *Ann. Phys.* **1903**, *10*, 105–179.
- Lorentz, H.A. Electromagnetic phenomena in a system moving with any velocity smaller than that of light. *Proc. R. Neth. Acad. Arts Sci.* **1904**, *6*, 809–831.
- Lorentz, H.A. *Theory of Electrons*, 2nd ed.; Dover: New York, NY, USA, 1952.
- Dirac, P.A.M. Classical theory of radiating electrons. *Proc. R. Soc. Lond. Ser. A Math. Phys. Sci.* **1938**, *167*, 148–169.
- Dirac, P.A.M. A new classical theory of electrons. *Proc. R. Soc. Lond. Ser. A Math. Phys. Sci.* **1951**, *209*, 291–296.
- Dymnikova, I. Image of the Electron Suggested by Nonlinear Electrodynamics Coupled to Gravity. *Particles* **2021**, *4*, 129–145. [CrossRef]
- Dirac, P.A.M. An extensible model of the electron. *Proc. R. Soc. Lond. Ser. A Math. Phys. Sci.* **1962**, *268*, 57–67.
- Boyer, R.H. Rotating fluid masses in general relativity. *Math. Proc. Camb. Philos. Soc.* **1965**, *61*, 527–530. [CrossRef]
- Boyer, R.H. Rotating fluid masses in general relativity. II. *Math. Proc. Camb. Philos. Soc.* **1966**, *62*, 495–501. [CrossRef]
- Righi, R.; Venturi, G. Nonlinear approach to electrodynamics. *Int. J. Theor. Phys.* **1982**, *21*, 63–82. [CrossRef]
- Rodrigues, W.A., Jr.; Vaz, J., Jr.; Recami, E. A Generalization of Dirac Non Linear Electrodynamics, and Spinning Charged Particles. *Found. Phys.* **1993**, *23*, 469–481. [CrossRef]
- Pope, T.; Hofer, W. Spin in the extended electron model. *Front. Phys.* **2017**, *12*, 128503. [CrossRef]
- Pope, T.; Hofer, W. A two-density approach to the general many-body problem and a proof of principle for small atoms and molecules. *arXiv* **2018**, arXiv:1801.06242.
- Newman, E.T.; Cough, E.; Chinnapared, K.; Exton, A.; Prakash, A.; Torrence, R. Metric of a rotating charged mass. *J. Math. Phys.* **1965**, *6*, 918–919. [CrossRef]
- Carter, B. Global structure of the Kerr family of gravitational fields. *Phys. Rev.* **1968**, *174*, 1559–1571. [CrossRef]
- Israel, W. Source of the Kerr metric. *Phys. Rev. D* **1970**, *2*, 641–646. [CrossRef]
- Burinskii, A.Y. Microgeons with spin. *Sov. Phys. JETP* **1974**, *39*, 23–42.
- López, C.A. Material and electromagnetic sources of the Kerr-Newman geometry. *Il Nuovo C. B (1971–1996)* **1983**, *76*, 9–27. [CrossRef]
- López, C.A. Extended model of the electron in general relativity. *Phys. Rev. D* **1984**, *30*, 313–316. [CrossRef]

24. Trümper, M. Einsteinsche Feldgleichungen für das axialsymmetrische stationäre Gravitationsfeld im Innern einer starr rotierenden idealen Flüssigkeit. *Z. Für Naturforschung* **1967**, *22*, 1347. [[CrossRef](#)]
25. Tiomno, J. Electromagnetic field of rotating charged bodies. *Phys. Rev. D* **1973**, *7*, 992–997. [[CrossRef](#)]
26. Burinskii, A.Y. The problem of the source of the Kerr–Newman metric: The volume Casimir effect and superdense pseudovacuum state. *Phys. Lett. B* **1989**, *216*, 123–126. [[CrossRef](#)]
27. Burinskii, A.; Elizalde, E.; Hildebrandt, S.R.; Magli, G. Regular sources of the Kerr–Schild class for rotating and nonrotating black hole solutions. *Phys. Rev. D* **2002**, *65*, 064039. [[CrossRef](#)]
28. Burinskii, A. Kerr–Newman electron as spinning soliton. *Int. J. Mod. Phys.* **2014**, *29*, 1450133. [[CrossRef](#)]
29. Burinskii, A. Gravitating lepton bag model. *J. Exp. Theor. Phys.* **2015**, *148*, 228–232. [[CrossRef](#)]
30. Burinskii, A. Gravitational strings beyond quantum theory: Electron as a closed heterotic string. *J. Phys. Conf. Ser.* **2012**, *361*, 012032. [[CrossRef](#)]
31. Burinskii, A. Stringlike structures in Kerr–Schild geometry. *Theor. Math. Phys.* **2013**, *177*, 1492–1504. [[CrossRef](#)]
32. Newman, E.T.; Janis, A.J. Note on the Kerr Spinning Particle Metric. *J. Math. Phys.* **1965**, *6*, 915–917. [[CrossRef](#)]
33. Gürses, M.; Gürsey, F. Lorentz covariant treatment of the Kerr–Schild geometry. *J. Math. Phys.* **1975**, *16*, 2385–2390. [[CrossRef](#)]
34. Kerr, R.P.; Schild, A. Some algebraically degenerate solutions of Einstein’s gravitational field equations. *Proc. Symp. Appl. Math.* **1965**, *17*, 199.
35. Ayon-Beato, E.; Garcia, A. Regular black hole in general relativity coupled to nonlinear electrodynamics. *Phys. Rev. Lett.* **1998**, *80*, 5056–5059. [[CrossRef](#)]
36. Ayon-Beato, E.; Garcia, A. New regular black hole solution from nonlinear electrodynamics. *Phys. Lett. B* **1999**, *464*, 25–29. [[CrossRef](#)]
37. Ayon-Beato, E.; Garcia, A. Non-singular charged black hole solution for non-linear source. *Gen. Rel. Grav.* **1999**, *31*, 629–633. [[CrossRef](#)]
38. Ayon-Beato, E.; Garcia, A. Four parametric regular black hole solution. *Gen. Rel. Grav.* **2005**, *37*, 635–641. [[CrossRef](#)]
39. Bronnikov, K.A. Regular magnetic black holes and monopoles from nonlinear electrodynamics. *Phys. Rev. D* **2001**, *63*, 044005. [[CrossRef](#)]
40. Breton, N. Born–Infeld black hole in the isolated horizon framework. *Phys. Rev. D* **2003**, *67*, 124004. [[CrossRef](#)]
41. Dymnikova, I. Regular electrically charged vacuum structures with de Sitter center in nonlinear electrodynamics coupled to general relativity. *Class. Quantum Gravity* **2004**, *21*, 4417–4428. [[CrossRef](#)]
42. Modesto, L.; Nicolini, P. Charged rotating noncommutative black holes. *Phys. Rev. D* **2010**, *82*, 104035. [[CrossRef](#)]
43. Balart, L.; Vagenas, E.C. Regular black hole metrics and the weak energy condition. *Phys. Lett. B* **2014**, *730*, 14–17. [[CrossRef](#)]
44. Balart, L.; Vagenas, E.C. Regular black holes with a nonlinear electrodynamics source. *Phys. Rev. D* **2014**, *90*, 124045. [[CrossRef](#)]
45. Toshmatov, B.; Ahmedov, B.; Abdurjabbarov, A.; Stuchlik, Z. Rotating regular black hole solution. *Phys. Rev. D* **2014**, *89*, 104017. [[CrossRef](#)]
46. Dymnikova, I.; Galaktionov, E. Basic Generic Properties of Regular Rotating Black Holes and Solitons. *Adv. Math. Phys.* **2017**, *2017*, 1035381. [[CrossRef](#)]
47. Born, M.; Infeld, L. Foundations of the new field theory. *Proc. R. Soc. Lond. Ser. A* **1934**, *144*, 425. [[CrossRef](#)]
48. Fradkin, E.S.; Tseytlin, A.A. Nonlinear electrodynamics from quantized strings. *Phys. Lett. B* **1985**, 123–130. [[CrossRef](#)]
49. Tseytlin, A.A. Vector field effective action in the open superstring theory. *Nucl. Phys. B* **1986**, *276*, 391–428. [[CrossRef](#)]
50. Sibeig, N.; Witten, E. String theory and noncommutative geometry. *J. High Energy Phys.* **1999**, *1999*, 32–92. [[CrossRef](#)]
51. Dymnikova, I. Spinning superconducting electrovacuum soliton. *Phys. Lett. B* **2006**, *639*, 368–372. [[CrossRef](#)]
52. Dymnikova, I.; Galaktionov, E. Regular rotating electrically charged black holes and solitons in nonlinear electrodynamics minimally coupled to gravity. *Class. Quantum Gravity* **2015**, *32*, 165015. [[CrossRef](#)]
53. Coleman, S. Classical lumps and their quantum descendants. In *New Phenomena in Subnuclear Physics: Part A*; Zichichi, A., Ed.; Springer Science & Business Media: Berlin/Heidelberg, Germany, 1977; p. 297.
54. Dymnikova, I. Mass, Spacetime Symmetry, de Sitter Vacuum, and the Higgs Mechanism. *Symmetry* **2020**, *12*, 634. [[CrossRef](#)]
55. Dymnikova, I. The cosmological term as a source of mass. *Class. Quantum Gravity* **2002**, *19*, 725–740. [[CrossRef](#)]
56. Dymnikova, I. Spacetime symmetry and mass of a lepton. *J. Phys. A Math. Theor.* **2008**, *41*, 304033. [[CrossRef](#)]
57. Englert, F.; Brout, R. Broken Symmetries and the Mass of Gauge Vector Mesons. *Phys. Rev. Lett.* **1964**, *13*, 321–323. [[CrossRef](#)]
58. Higgs, P.W. Broken symmetries and the masses of gauge bosons. *Phys. Rev. Lett.* **1964**, *13*, 508–509. [[CrossRef](#)]
59. Guralnik, G.S.; Hagen, C.R.; Kibble, T.W.B. Global conservation laws and massless particles. *Phys. Rev. Lett.* **1964**, *13*, 585–587. [[CrossRef](#)]
60. Quigg, C. *Gauge Theories of the Strong, Weak and Electromagnetic Interactions*; Addison-Wesley Publishing Company: Redwood City, CA, USA, 1983.
61. Weinberg, S. *The Quantum Theory of Fields II*; Cambridge University Press: Cambridge, UK, 1996.
62. Dymnikova, I.; Galaktionov, E. Regular rotating de Sitter–Kerr black holes and solitons. *Class. Quantum Grav.* **2016**, *33*, 145010. [[CrossRef](#)]
63. Dymnikova, I.; Sakharov, A.; Ulbricht, J. Minimal Length Scale in Annihilation. *arXiv* **2009**, arXiv:0907.0629.
64. Dymnikova, I.; Sakharov, A.; Ulbricht, J. Appearance of a minimal length in e^+e^- annihilation. *Adv. High Energy Phys.* **2014**, *2014*, 707812. [[CrossRef](#)]

65. Dymnikova, I.; Galaktionov, E. Dynamics of Electromagnetic Fields and Structure of Regular Rotating Electrically Charged Black Holes and Solitons in Nonlinear Electrodynamics Minimally Coupled to Gravity. *Universe* **2019**, *5*, 205. [[CrossRef](#)]
66. Chandrasekhar, S. *The Mathematical Theory of Black Holes*; Clarendon Press: New York, NY, USA, 1983.
67. Dymnikova, I. The Higgs Mechanism and Spacetime Symmetry. *Universe* **2020**, *6*, 179. [[CrossRef](#)]
68. Landau, L.D.; Lifshitz, E.M. *Electrodynamics of Continued Media*; Pergamon Press: Oxford, UK, 1993.
69. Dymnikova, I.; Galaktionov, E.; Tropp, E. Existence of electrically charged structures with regular center in nonlinear electro-dynamics minimally coupled to gravity. *Adv. Math. Phys.* **2015**, *2015*, 496475. [[CrossRef](#)]
70. Dymnikova, I. Electromagnetic source for the Kerr–Newman geometry. *Int. J. Mod. Phys. D* **2015**, *24*, 1550094. [[CrossRef](#)]
71. Dymnikova, I. Origin of the magnetic momentum for regular electrically charged objects described by nonlinear electro-dynamics coupled to gravity. *Intern. J. Mod. Phys. D* **2019**, *28*, 1950011. [[CrossRef](#)]
72. Hawking, S.W.; Ellis, G.F.R. *The Large Scale Structure of Space-Time*; Cambridge University Press: Cambridge, UK, 1973.
73. Dymnikova, I. De Sitter–Schwarzschild black hole: Its particlelike core and thermodynamical properties. *Int. J. Mod. Phys. D* **1996**, *5*, 529–540. [[CrossRef](#)]
74. Bassett, B.A.; Kunz, M.; Silk, J.; Ungarelli, C. A late-time transition in the cosmic dark energy? *Mon. Not. R. Astron. Soc.* **2002**, *336*, 1217–1222. [[CrossRef](#)]
75. Corasaniti, P.S.; Kunz, M.; Parkinson, D.; Copeland, E.J.; Bassett, B.A. Foundations of observing dark energy dynamics with the Wilkinson Microwave Anisotropy Probe. *Phys. Rev. D* **2004**, *70*, 083006. [[CrossRef](#)]
76. Licata, I.; Chiatti, L. Archaic Universe and Cosmological Model: “Big-Bang” as Nucleation by Vacuum. *Intern. J. Theor. Phys.* **2010**, *49*, 2379–2402. [[CrossRef](#)]
77. Suzuki, N.; Rubin, D.; Lidman, C.; Aldering, G.; Amanullah, R.; Barbary, K.; Barrientos, L.F.; Botyanszki, J.; Brodwin, M.; Connolly, N.; et al. The Hubble Space Telescope Cluster Supernova Survey: Improving the Dark Energy Constraints and Building an Early-Type-Hosted Supernova Sample. *Astrophys. J.* **2012**, *746*, 85. [[CrossRef](#)]
78. Ade, P.A.; Aikin, R.W.; Barkats, D.; Benton, S.J.; Bischoff, C.A.; Bock, J.J.; Brevik, J.A.; Buder, I.; Bullock, E.; Dowell, C.D.; et al. Detection of B-Mode Polarization at Degree Angular Scales by BICEP2. *Phys. Rev. Lett.* **2014**, *112*, 241101. [[CrossRef](#)] [[PubMed](#)]
79. Anderson, L.; Aubourg, E.; Bailey, S.; Beutler, F.; Bhardwaj, V.; Blanton, M.; Bolton, A.S.; Brinkmann, J.; Brownstein, J.R.; Burden, A.; et al. The clustering of galaxies in the SDSS-III Baryon Oscillation Spectroscopic Survey: Baryon acoustic oscillations in the Data Releases 10 and 11 Galaxy samples. *Mon. Not. R. Astron. Soc.* **2014**, *441*, 24–62. [[CrossRef](#)]
80. Sahni, V.; Shafiello, A.; Starobinsky, A.A. Model-independent Evidence for Dark Energy Evolution from Baryon Acoustic Oscillations. *Astrophys. J. Lett.* **2014**, *793*, L40. [[CrossRef](#)]
81. Rivera, A.B.; Garcia-Farieta, J.E. Exploring the Dark Universe: Constraint on dynamical dark energy models from CMB, BAO and Growth Rate Measurements. *Int. J. Mod. Phys. D* **2019**, *28*, 1950118. [[CrossRef](#)]
82. Dymnikova, I. The fundamental roles of the de Sitter vacuum. *Universe* **2020**, *6*, 101. [[CrossRef](#)]

Disclaimer/Publisher’s Note: The statements, opinions and data contained in all publications are solely those of the individual author(s) and contributor(s) and not of MDPI and/or the editor(s). MDPI and/or the editor(s) disclaim responsibility for any injury to people or property resulting from any ideas, methods, instructions or products referred to in the content.